

See discussions, stats, and author profiles for this publication at: <https://www.researchgate.net/publication/228555308>

# Isomerization and Polymerization of Phospholipids with Terminal Diene Groups in Supported Films

ARTICLE *in* THE JOURNAL OF PHYSICAL CHEMISTRY B · JANUARY 1999

Impact Factor: 3.3 · DOI: 10.1021/jp9819083

---

CITATIONS

16

---

READS

9

3 AUTHORS, INCLUDING:



**Hans Binder**

University of Leipzig

126 PUBLICATIONS 2,630 CITATIONS

SEE PROFILE



**Bernd Kohlstrunk**

University of Leipzig

14 PUBLICATIONS 545 CITATIONS

SEE PROFILE

# Isomerization and Polymerization of Phospholipids with Terminal Diene Groups in Supported Films

H. Binder,\* A. Anikin,<sup>†</sup> and B. Kohlstrunk

Universität Leipzig, Institut für Experimentelle Physik I, Linnèstrasse 5, D-4103 Leipzig, Germany

Received: April 17, 1998; In Final Form: November 2, 1998

Diene groups in the terminal position of the lipid acyl chains undergo an irreversible *cis* → *trans* isomerization when lipid films are incubated on a solid support under an atmosphere which is adjusted to a relative humidity (RH) in the range 20% < RH < 100%. In general, isomerization and polymerization can be modulated by RH, temperature, and the phase state of the lipid. Under nearly dry conditions or in water excess the isomerization is paralleled by the spontaneous polymerization of the diene groups. Alternatively, polymerization can be realized by UV irradiation. This process is accompanied and/or preceded by the *cis* → *trans* photoisomerization of the terminal diene groups. The kinetics of isomerization and polymerization are investigated by means FTIR spectroscopy using selected absorption bands of the diene groups. The lipid films are characterized before and after polymerization. Polymerization of solid lipid phases destroys the crystalline packing of the acyl chains and causes conformational defects between the methylene units. Nevertheless it gives rise to polymerized multilayers which are well-oriented on the solid support. The analysis of the kinetic data gives rise to the conclusion that the degree of molecular ordering within the hydrophobic region of the lipid aggregates controls the isomerization and polymerization reactions. Both processes are assumed to proceed via an intermediate twisted conformation.

## 1. Introduction

The development of relative simple synthetic membrane analogues has been prompted by the idea to circumvent the inherent complexities of the biological ensemble. Polymerizable lipids attract considerable interest because they raise the prospect to develop biocompatible materials with, for example enhanced stability, controllable permeability, or size. Several polymerizable fragments as, for example diacetylene, diene, triene, styrene, or methacryle groups can be incorporated into lipid analogues to synthesize the precursors of the polymer.<sup>1–3</sup> It turns out that diene groups represent a suitable choice because of their relatively high stability and because they cause relatively small perturbations of membrane structure.<sup>3–5</sup> Furthermore, diene groups enable a high variability in the design of polymerizable lipids because their position can be varied along the acyl chains to modulate the properties of the monomeric and polymerized membranes. Last but not least, different headgroups, such as phosphatidylcholine (PC) or phosphatidylethanolamine (PE), can be attached to fragments with dienoyl fatty acid residues to vary the properties of the polar/apolar interface.

Our preceding paper has been devoted to the lyotropic phase behavior of lipids with terminal diene groups which were investigated mainly by means of FTIR spectroscopy using the ATR technique.<sup>6</sup> One logical continuation of this study would be the study of the polymerization products obtained from the lipid films in the different phase states. We found that the polyreaction of the terminal diene groups in lipid films is closely related to a rotation about the inner double bond. Interestingly this *cis* → *trans* isomerization of the diene group was not observed when the lipid has been stored in a nonaggregated state. Therefore, the main purpose of the present paper is to systematically study the factors which affect isomerization and

polymerization to get insight into possible reaction paths and, thus, to control these processes.

Environmental effects on molecular relaxation processes, interactions and mobility are often reflected in the overall course and product distribution of reactions. It is known that, for example factors which are relatively unimportant in solution can dominate reactivity in an ordered molecular environment as monolayers<sup>7</sup> or crystals.<sup>8,9</sup> In particular, *cis* → *trans* photoisomerization and polymerization are such processes with a large medium sensitivity.<sup>10</sup>

In a general frame, the “environmental behavior” of unsaturated organic compounds is of fundamental interest for the understanding of the nature of chemical bonds. Reactions of amphiphilic butadienes in layered structures were studied, but only little has been reported on photoreactivity of these compounds in bulk multilayers, and the reaction paths could not be identified.<sup>8</sup> As has been stated previously, polymerization in organized molecular assemblies presents several novel aspects which do not allow the straightforward application of the theories developed for homogeneous, bulk, and emulsion polymerizations.<sup>11</sup>

The present paper deals with the factors which affect isomerization and polymerization of terminal diene groups in lipid aggregates. The knowledge of these factors is of practical importance in a 2-fold respect. On one hand, they define the conditions of stability of terminal diene groups. On the other hand, they allow us to control the transformation from the *cis* into the *trans* isomer. The kinetics of spontaneous and UV-induced conversions are investigated in order to get insight into the reaction mechanism by means of infrared (IR) spectroscopy using selected absorption bands of the diene groups. Furthermore, we compare selected molecular properties of the films before and after polymerization.

The lipids were investigated as films spread on a plane solid support. This choice is motivated by several reasons: First, the use of an ATR crystal as supporting surface enables to follow

<sup>†</sup> Lomonossow State Academy of Fine Chemical Technology, Moscow, Russia.

\* To whom correspondence should be addressed. E-mail: binder@rz.uni-leipzig.de. Fax: +49-341-9732479.

**TABLE 1: Assignments of Selected Absorption Bands of the Terminal Diene Groups of *cis* and *trans* Isomers of DTDPC and of Penta and Hexadiene<sup>a</sup>**

group vibration	mode	symbol	wavenumber/cm <sup>-1</sup>			
			DTDPC		penta- and hexadiene	
			cis	trans	cis	trans
C–H stretching	=CH <sub>2</sub> antisymmetric	$\nu_{as}(=CH_2)$	3086–3085	3086–3085	3086 m	3089 m
	=CH <sub>2</sub> symmetric	$\nu_s(=CH_2)$	3010–3009	3009		3010 m
	=CH	$\nu(CH)$	3048		3053 w	
methyl bending	=CH	$\nu(CH)$	3029 <sup>b</sup>	3037	3023 br <sup>†</sup>	3039–3036 m
	=CH <sub>2</sub>	$\delta(CH_2)$	1434	x	1433 s	1413 m
	=CH out of plane	$\gamma_w(CH)$	996–997 <sup>†</sup>	1002	996 m <sup>†</sup>	1003 vs
methyl and methyne wagging	=CH out of plane	$\gamma_w(CH)$		951	955 w	949 m
	=CH <sub>2</sub> wagging	$\gamma_w(=CH_2)$	901–903 <sup>↓</sup>	898–900	908–898 br <sup>↓</sup>	899 vs
	=CH out of plane, cis	$\gamma_w(CH)_{cis}$	784	x	773	
C=C double bond stretching	C=C–C=C symmetric	$\nu_s(C=C)$	1644 <sup>†</sup>	1653	1647 m <sup>†</sup>	1655 s
	C=C–C=C antisymmetric	$\nu_{as}(C=C)$	1593 <sup>†</sup>	1603	1596 m <sup>†</sup>	1604 m

<sup>a</sup> DTDPC membranes ( $T = 25^\circ\text{C}$ , RH = 50%), liquid penta- and hexadiene, band positions are resolved to whole wavenumbers and assignments are taken from ref 17. <sup>b</sup> Arrows illustrate frequency shift upon *cis* → *trans* isomerization. <sup>c</sup> br = broad, m = medium, s = strong, vs = very strong, w = weak.

the kinetics of UV polymerization directly by IR spectroscopy. Second, the sample can be exposed to an atmosphere of definite relative humidity (RH) to hydrate the lipids in a definite way. Third, the lipid film can be illuminated uniformly by UV light. And ultimately, the use of polarized IR radiation yields the macroscopic orientation of the molecules within the films. Besides these methodological arguments supported polymerized lipid films possess properties as, for example a high stability and a large, available surface which may be advantageous for the development of biocompatible materials in perspective.

## 2. Materials and Methods

**Materials.** 1,2-Bis(11,13-tetradecadienoyl)-*sn*-glycero-3-phosphorylcholine (DTDPC) and 1,2-bis(11,13-tetradecadienoyl)-*sn*-glycero-3-phosphorylethanolamine (DTDPE) were synthesized as described previously.<sup>6,12</sup> The synthesis of 1,2-di-(9*cis*,11*trans*-octadecadienoyl)-*sn*-glycero-3-phosphocholine (9,11-DODPC) was described in reference 13. Stock solution (chloroform–methanol: 3:1 v/v; 5 mg/mL) of the lipids were used for sample preparation. *trans*-Hexatriene (99% purity) and *cis*- (98%) and *trans*- (97%) pentadiene were purchased from Aldrich (Steinheim, Germany).

**Sample Preparation and FTIR Measurements.** Samples were prepared by spreading 100  $\mu\text{L}$  of the stock solution on a ZnSe-attenuated total reflection (ATR) crystal and evaporating the solvent. The ATR crystal was mounted on a horizontal holder unit which allows to realize a definite relative humidity (RH) and temperature ( $T$ ) at the crystal surface using a moisture regulating device (HumiVar, Leipzig).<sup>5</sup> During the investigations the samples were kept in an anaerobic N<sub>2</sub> atmosphere. To make possible UV polymerization experiments, the cover of the sample cell has been modified with a quartz window which enables the uniform illumination of the ATR-surface coated with the lipid using a UV lamp (4 W, distance to the lipid film  $\sim 3$  cm). In some experiments, the UV intensity has been attenuated to  $\sim 30\%$  of the original value by inserting a wire grid between the lamp and the quartz window. Measurements in excess water were realized by injecting degassed micropore water into the sample cell.

Polarized IR measurements were performed using a BioRad FTS-60a Fourier transform infrared spectrometer (Digilab, MA) equipped with a polarizer as described previously.<sup>6</sup> For measurements under equilibrium conditions, 128 scans were accumulated for each polarized spectrum  $A_{||}(\nu)$  and  $A_{\perp}(\nu)$  corresponding to light which is polarized parallel and perpendicularly with respect to the plane of incidence. Temperature scans were realized in steps of 1–2 K at constant relative humidity. For kinetic measurements a series of spectra with a progressively

increasing number of accumulations were recorded, namely, (4 pairs of polarized spectra with 32 scans each), (4  $\times$  64), (4  $\times$  128), (4  $\times$  256) .... In this way the time interval between subsequent spectra increases from  $<1.5$  min within the first 20 min up to, for example  $>30$  min after 5 h. In each measuring cycle the chronological order of perpendicular and parallel orientations of the polarizer alternate to minimize artifacts which could be caused by time dependent changes of the absorbance. This type of measurements starts ( $t = 0$ ) when the UV lamp was switched on (polymerization) or, alternatively, when the sample was exposed to the respective conditions ( $T$  and RH, spontaneous isomerization and polymerization, see below).

The polarized absorbance spectra has been analyzed in terms of the IR order parameter  $S_{IR}$  and center of gravity COG of selected absorption bands as described in the accompanying paper.<sup>6</sup> The molar fractions of *cis* and *trans* isomers have been determined from the integral absorbances of selected vibrational modes of the diene groups (vide infra). To eliminate the effect of macroscopic molecular ordering, we used the combination  $A = A_{||} + 2.55A_{\perp}$  where  $A_{||}$  and  $A_{\perp}$  denote the polarized absorbances (see ref 6).

The spectra of liquid hexatriene and pentadiene are recorded in the transmission mode using a liquid cell equipped with ZnSe windows and a 25  $\mu\text{m}$  spacer in between.

## 3. Experimental Results

***cis* → *trans* Isomerization.** The diene groups in freshly prepared DTDPC membranes are expected to constitute a 20:1 mixture of *cis* and *trans* isomers according to the composition of 11,13-tetradecadienoic acid used for the synthesis.<sup>12</sup> Indeed, most of the IR absorption bands of the diene groups resemble closely that of *cis*-1,3-pentadiene the IR spectra of which have been recorded for comparison (Table 1; see also ref 14). The detailed inspection of the  $\nu_{as}(C=C)$  mode of the lipid reveals a doublet, the weaker left-hand component band of which can be assigned to the small fraction of *trans* isomers in analogy to the respective band observed at the same position in the spectrum of *trans*-1,3-pentadiene.

When storing the lipid films overnight ( $T > 25^\circ\text{C}$ , under N<sub>2</sub> atmosphere) the spectral pattern of the diene groups changes considerably. Besides variations in intensity (e.g., increase of  $\gamma_w(=CH)$  and decrease of  $\gamma_w(=CH_2)$ ) the most bands shift by several wavenumbers. Interestingly their new positions match amazingly well with that of *trans*-pentadiene and *trans*-hexadiene (Table 1). For example, the absorbance of the left-hand component band of the  $\nu_{as}(C=C)$  mode increases, whereas its right-hand component band nearly completely disappears. According to the spectral pattern of dienes (cf. Table 1) the

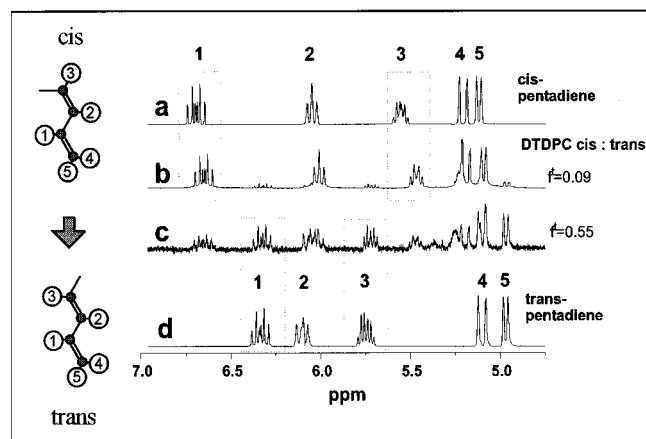


**Figure 1.**  $^1\text{H}$  NMR spectra of (spectrum a) *cis*- and (spectrum d) *trans*-pentadiene and of (spectrum b) “fresh” DTDPC which was taken from the stock solution, dried and immediately resolubilized in  $\text{CDCl}_3$  and of (spectrum c) DTDPC which was stored as film on solid substrate at RH = 80% and 50 °C for 12 h and subsequently dissolved in  $\text{CDCl}_3$ . Proton signals are assigned as illustrated in the left part of the figure in correspondence with ref 15. The integral intensities of the proton resonances 1 or 3 yield the mol fractions of the trans isomers (e.g.,  $f^t = I(6.34 \text{ ppm}) / (I(6.34 \text{ ppm}) + I(6.65 \text{ ppm}))$  for proton 1) given at spectra b and c (SE:  $\pm 0.05$ ).

frequency shift of the  $\gamma_{\text{w}}(\text{CH})$  mode and the disappearance of the weak  $\gamma_{\text{w}}(\text{CH})_{\text{cis}}$  band at  $784 \text{ cm}^{-1}$  are characteristic for a *cis*  $\rightarrow$  *trans* isomerization. Furthermore, the presence of isobestic points (e.g., at  $1648 \text{ cm}^{-1}$  for  $\nu_{\text{as}}(\text{C}=\text{C})$ ; at  $1599 \text{ cm}^{-1}$  for  $\nu_{\text{s}}(\text{C}=\text{C})$  and at  $997$  for  $\gamma_{\text{w}}(\text{CH})$ ) suggests a transformation between two states. The invariance of the integral absorbance of the  $\text{C}=\text{C}$  stretching bands indicates that the conjugated double bonds do not decompose during samples storage (except under special cases which are discussed below).

Further evidence of this latter finding has been obtained from the UV transmission spectra of lipid membranes prepared on quartz slides. The position, shape and intensity of the electronic absorption band of the diene group centered at  $\sim 235 \text{ nm}$  does not change upon storage of the membranes under similar conditions as applied to the IR samples. Note that decomposition of the diene groups, e.g., upon UV-induced polymerization, leads to the complete disappearance of the UV and IR absorption bands under discussion (see below). Moreover, the product remains soluble in organic solvents and, thus, polymerization can be excluded because the polymer was found to be insoluble.

For  $^1\text{H}$  NMR spectroscopy, the DTDPC films after incubation were dissolved in  $\text{CDCl}_3$  by rinsing the ATR crystal by the solvent. Comparison of the corresponding  $^1\text{H}$  NMR spectra and those of DTDPC taken from the original stock solution with the NMR spectra of the reference substances, *cis*- and *trans*-pentadiene, gives final evidence that in membranes the *cis* isomers of the diene groups transform spontaneously into the *trans* isomers (Figure 1). The fraction of the *trans* isomer  $f^t$  was obtained from the integrated intensities of selected proton resonances.

This value was used to determine the ratio of the extinction coefficients of the  $\nu_{\text{as}}(\text{C}=\text{C})$  mode of the *trans* and *cis* isomers,  $g_{\text{tc}} = (\epsilon_{\text{t}}(\nu_{\text{as}}(\text{C}=\text{C}))/\epsilon_{\text{c}}(\nu_{\text{as}}(\text{C}=\text{C}))) = (1 - f^t)/f^t \cdot (A_{1603}/A_{1593}) = 1.2 \pm 0.4$ , where  $A_{1603}$  and  $A_{1593}$  denote the base-line-corrected integral absorbances of the  $\nu_{\text{as}}(\text{C}=\text{C})$  component bands. An analogous estimation yields for the  $=\text{CH}$  wagging mode  $(\epsilon_{\text{t}}(\gamma_{\text{w}}(\text{CH}))/\epsilon_{\text{c}}(\gamma_{\text{w}}(\text{CH}))) = 1.8 \pm 0.2$ . One can use, vice versa, the  $g_{\text{tc}}$  values to determine  $f^t$  by means of IR spectroscopy and, thus, to study the kinetics of *cis*  $\rightarrow$  *trans* isomerization in lipid films at different conditions. Note that the  $\nu_{\text{as}}(\text{C}=\text{C})$  component

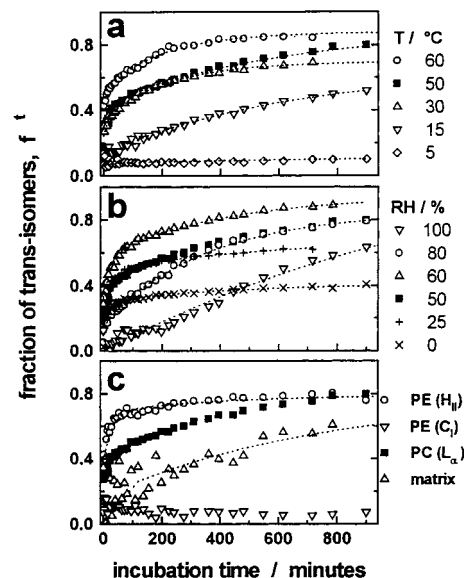


**Figure 2.** Fraction of *trans* isomers  $f^t(t)$  as a function of incubation time of diene lipids in films at different conditions: (part a) DTDPC at RH = 50% and different temperatures; (part b) DTDPC at  $T = 50$  °C and different RH; (part c) of pure DTDPC, of a DMPC/DTDPC mixture (8:1 mol/mol), of DTDPE in the  $\text{H}_{\text{II}}$  phase ( $T = 50$  °C and RH = 50%) and of DTDPE in the crystalline  $\text{C}_1$  state ( $T = 15$  °C, RH = 50%). The dotted lines represent fits according to eq 1 (see also Table 2). The error of the fraction data is  $\sim \pm 0.1$ .

bands are well separated and nearly free of overlapping bands but of weak intensity. The precision of the corresponding fraction data is  $\delta f^t \approx \pm 0.1$ . In contrast, the  $=\text{CH}$  wagging bands are more intense but less resolved (cf. Figure 5). The latter feature was used for the determination of  $f^t$  of DTDPC in excess water and of DTDPC diluted within a DMPC matrix because in these cases the  $\nu_{\text{as}}(\text{C}=\text{C})$  band can hardly be analyzed owing to its low intensity or its strong overlap with the  $\nu_2$  band of water.

In general, the time courses of  $f^t$ ,  $f^t(t) = A_{1603}(t)/(g_{\text{tc}}A_{1603}(t) + A_{1593}(t))$ , possess multiphase character with a fast initial rise followed by a slower increase at longer incubation times (cf. Figure 2). They could be well-fitted empirically using

$$f^t(t) = f_{\infty} - \{f_{30}\exp(-t/30 \text{ min}) + f_{\text{L}}\exp(-t/\tau_{\text{L}})\} \quad (1)$$

The preexponential factors  $f_{30}$  and  $f_{\text{L}}$  give the amount of  $f^t$  which converts with a time constant of 30 min and of  $\tau_{\text{L}} > 30$  min, respectively. The former correlation time was set constant whereas the latter was adjusted to fit the experimental data. It amounts typically to values  $\tau_{\text{L}} \approx 200\text{--}1000$  min.  $f_{\infty}$  denotes the final yield of *trans* isomers extrapolated to infinite incubation times,  $t \rightarrow \infty$ . It increases with temperature and RH (at RH < 50%, Table 2). The difference  $(f_{\infty} - f_{\text{L}})$  represents a measure of the amount of *cis* isomers which can be obtained at relatively short times. When the relative humidity is increased at constant temperature, this parameter passes through a maximum in the intermediate RH range in contrast to its temperature behavior at constant RH where  $(f_{\infty} - f_{\text{L}})$  varies monotonically.

To quantify the effective rate of *cis*  $\rightarrow$  *trans* isomerization, we determined the incubation time  $t_{45}$  (and  $t_{60}$ ), which is necessary for a 45% (60%) conversion of monomeric DTDPC from the curves shown in parts a and b of Figure 2. The Arrhenius plot of these quantities (i.e.,  $\ln(1/t_{45,60})$  vs  $1/T$ ) yields activation energies of  $E_{\text{A}} = 65 \text{ kJ/mol}$  (45 kJ/mol).



**TABLE 2: Kinetic Analysis of cis  $\rightarrow$  trans Isomerization in Films of Diene Lipids at Different Conditions<sup>a,b</sup>**

	$T/^{\circ}\text{C}$					
	5	15	30	50	60	
$f_{\infty}$	0.11	0.63	0.68	0.87	0.85	
$f_{\infty} - f_{\text{L}}$	0.01	0.07	0.19	0.31	0.37	
RH/%						
	<1	25	50	60	80	99<
$\Pi/\text{GPa}^{\text{c}}$	>0.69	0.207	0.103	0.076	0.033	0.001>
$f_{\infty}$	0.40	0.67	0.87	0.93	0.83	$0.85 \pm 0.20$
$f_{\infty} - f_{\text{L}}$	0.29	0.49	0.43	0.58	0.18	0
system						
	DTDPE		DTDPC		matrix	
$f_{\infty}$	0.77		0.87		$0.77 \pm 0.2$	
$f_{\infty} - f_{\text{L}}$	0.68		0.31		$0.17 \pm 0.2$	

<sup>a</sup> Fit of eq 1 to the data shown in Figure 2.  $f_{\infty}$  and  $(f_{\infty} - f_L)$  denote the fractions of trans isomers formed at long and short incubation times, respectively. <sup>b</sup> Standard errors of  $f_{\infty}$  and  $(f_{\infty} - f_L)$ :  $\pm 0.1$  (if not stated otherwise). <sup>c</sup> Vapor pressure:  $\Pi = (-RT/\nu_W)\ln(RH/100)$ ;  $R$ , gas constant;  $\nu_W = 1.8 \times 10^{-5} \text{ m}^3 \text{ mol}^{-1}$ , molar volume of water.<sup>5</sup>

The RH dependence can be interpreted in terms of the vapor pressure,  $\Pi$  (see Table 2 for definition), acting on the lipid aggregates. With decreasing RH, the vapor pressure increases leading to a progressive dehydration of the lipids and, as a result, to its compression.<sup>5,16</sup> Consequently, one can calculate an activation volume  $V_A$ , using the incubation times  $t_{45}$  ( $t_{60}$ ) which are determined at RH  $\approx$  99%, 80% and 60% (at  $T = 50^\circ\text{C}$ ) and plotting  $\ln(1/t_{45,60})$  as a function of  $\Pi$  (not shown). The slope of the linear regression of this representation yields  $V_A = -1.4 \text{ cm}^3/\text{mol}$  ( $-1.0 \text{ cm}^3/\text{mol}$ ).

The total absorbance of the  $\nu_{\text{as}}(\text{C}=\text{C})$  bands of both isomers,  $I_{\text{tot}} = (g_{\text{te}}A_{1603} + A_{1593})$ , was used to check the integrity of the diene groups during incubation (not shown). Whereas  $I_{\text{tot}}$  remains constant at 99%  $>$  RH  $\geq$  20%, it progressively decreases when the sample was held under relatively dry or humid  $\text{N}_2$  atmosphere (RH  $<$  20% and RH  $\approx$  99%) or in excess water ( $T = 50^\circ\text{C}$ , see below). Obviously in these cases the diene groups decompose slowly.

When incubating the PE analogue DTDPE under similar conditions, it converts either faster ( $T = 50^\circ\text{C}$ ) or slower ( $T = 15^\circ\text{C}$ ) than DTDPC (Figure 2, part c). In the former case DTDPE exists in the inverted hexagonal phase ( $\text{H}_{\text{II}}$ ).<sup>6</sup> The  $\text{H}_{\text{II}}$  structure of the PE is characterized by slightly more disordered acyl chains in comparison with the fluid-lamellar phase ( $\text{L}_\alpha$ ) of the PC because of the increased free volume existing in the hydrophobic core of the inversely curved aggregates. At  $T = 15^\circ\text{C}$  DTDPE exist in the crystalline  $\text{C}_1$  state with highly ordered acyl chains<sup>6</sup> in contrast to DTDPC which is still in the  $\text{L}_\alpha$  phase (see below). We conclude that the phase state of the lipid affects the isomerization significantly probably because of the different fluidity within the hydrophobic region of the lipid assemblies.

Direct interactions between the diene groups of dienic lipids were suggested to cause the stacking of these groups in the gel state.<sup>17</sup> To answer the question whether the cis  $\rightarrow$  trans isomerization process requires specific interactions between the diene groups we incubated a 8:1 (mol/mol) mixture of DMPC and DTDPC. Both lipids can be assumed to mix almost randomly because of the equal number of carbons in the acyl chains ( $n_{\text{eff}} = 14$ ). Hence, the number of direct contacts between diene groups in the mixed bilayer is expected to be much smaller in comparison with pure DTDPC bilayers. It turns out that the isomerization is essentially not affected by the dilution of diene groups within a matrix of saturated acyl chains (Figure 2, part

c). The slightly slower conversion in comparison with pure DTDPC is probably caused by the higher molecular ordering within the DMPC matrix.

When storing the lipid isomers (cis or trans) dissolved in an organic solvent their IR spectra remain unchanged for months. We conclude that the hydrophobic core of lipid bilayers is of decisive importance to promote the isomerization process.

**UV-Induced Polymerization and Isomerization.** To study the kinetics of UV polymerization, the lipid films were irradiated by an UV lamp which was placed directly above the ATR crystal. Typical time-dependent spectra of selected absorption bands of the diene groups of DTDPC are shown in Figure 3. During UV illumination, these bands vanish completely, indicating a reaction of the conjugated double bonds. Simultaneously a new mode appears at  $\sim 968 \text{ cm}^{-1}$ , which can be attributed to the  $=\text{CH}$  wagging mode of an isolated trans  $-\text{CH}=\text{CH}-$  unit,  $\gamma_{\text{W}}(\text{CH})_{\text{P}}$ , as is present, for example in 1,4-*trans*-polybutadienes.<sup>8,18</sup> The  $\gamma_{\text{W}}(\text{CH})_{\text{P}}$  band protrudes clearly in the spectrum of the ethanolamine analogue of DTDPC, where no  $\text{N}^+\text{CH}_3$  stretching band ( $\sim 967 \text{ cm}^{-1}$ ) interferes with the  $\gamma_{\text{W}}(\text{CH})_{\text{P}}$  mode (Figure 3). Since the disappearance of the diene bands must not necessarily be due to a polyreaction but can also be caused by, for example dimerization, additional proof for polymer formation has been obtained by the inability to dissolve the product in organic solvents (e.g., chloroform, methylene chloride, methanol, and ethanol).<sup>3,4</sup> This property suggests polymeric units of more than 50 lipids because smaller oligomeric units has been found to be soluble.<sup>4</sup> Note that the irradiated films could be removed from the solid support only mechanically after intensive rubbing. This finding gives further evidence for the polymerization of the terminal diene groups where the particular type of links between the acyl chains remains however speculative (see below).

The detailed inspection of the time-dependent spectra in the ranges of the  $\nu_{\text{as}}(\text{C}=\text{C})$  and  $\gamma_{\text{W}}(\text{CH})$  modes reveals an interesting phenomenon. Before these bands disappear, their shapes and positions change in an analogous fashion as observed upon cis  $\rightarrow$  trans isomerization (compare Table 1 and Figure 3). In particular, the  $\nu_{\text{as}}(\text{C}=\text{C})$  and  $\gamma_{\text{W}}(\text{CH})$  bands of the trans isomer appear and increase in intensity immediately after switching on the UV lamp. This process is paralleled by the intensity decrease of the subbands which are assigned to the cis isomer. We conclude that UV-induced cis  $\rightarrow$  trans isomerization of the terminal diene groups precedes and/or accompanies polymerization.

The inset in Figure 3 shows that similar spectral effects can be observed upon UV irradiation of 1,2-di-(9-*cis*,11-*trans*-octadecadienoyl)-*sn*-glycero-3-phosphocholine (9,11-DODPC) possessing diene groups in the middle of the acyl chains.<sup>13</sup> In contrast to the behavior of the terminal diene groups no cis  $\rightarrow$  trans isomerization has been observed in 9,11-DODPC membranes when stored at similar conditions as used for DTDPC (see above). However, upon UV irradiation, a  $\gamma_{\text{W}}(\text{CH})$  mode protruding as a shoulder at  $\sim 946 \text{ cm}^{-1}$  is replaced by a strong feature at  $\sim 984 \text{ cm}^{-1}$  which can be assigned to the  $\gamma_{\text{W}}(\text{CH})$  band of the (trans,trans) isomer. Obviously, cis  $\rightarrow$  trans isomerization of diene groups can be also induced by UV irradiation when the diene groups are inserted in the middle of the polymethylene chains by means of (1,4)-disubstitution.

The polyreaction in DTDPC and DTDPE can quantitatively be followed using the absorbance of the  $\nu_{\text{as}}(\text{C}=\text{C})$  component bands to calculate the fraction tetradecadienoyl chains with diene groups in the trans and cis configuration  $F^{\text{c}}$  and  $F^{\text{t}}$ , respectively, and the mol fraction of polymerized acyl chains  $F^{\text{P}}$ , as a function

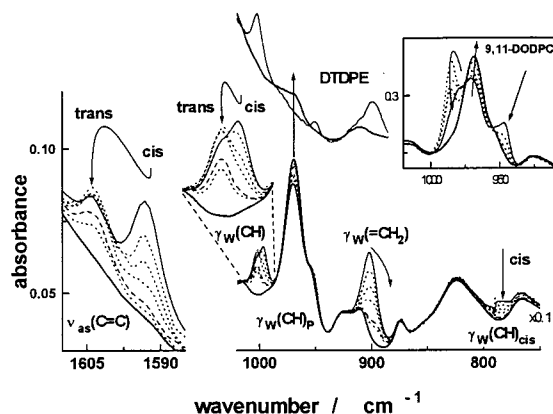


**Figure 3.** Selected regions of the infrared absorbance spectra of DTDPC (below), of DTDPE (above) and of 9,11-DODPC (inset) during UV irradiation. The irradiation time (minutes) was  $t = 0$  (monomer, solid line), 1, 3, 7, 15 (dotted lines), 12 (dashed line), and 30 (polymer, thick solid line). The arrows illustrate characteristic changes of the absorption bands originating from the diene groups.

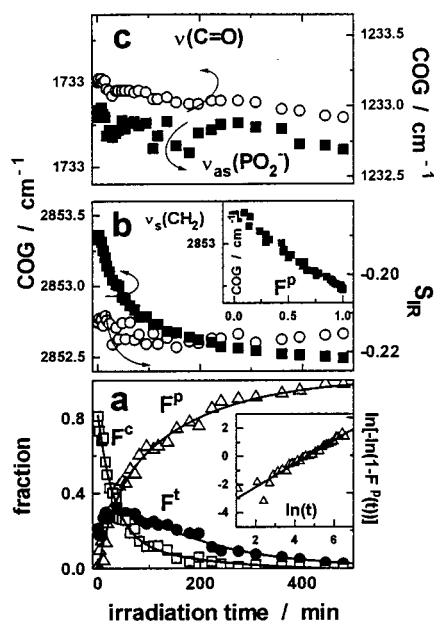


**Figure 4.** Fraction of trans- and cis isomers and of polymeric DTDPC (part a;  $F^T$ ,  $F^C$ , and  $F^P$ , respectively) and spectral parameters (parts b and c) as a function of UV irradiation time. The lines represent biexponential functions which are fitted to the data with  $\tau_1 = 172$  min and  $\tau_2 = 31$  min (see also Table 3). Part b depicts the center of gravity (COG) and IR order parameter ( $S_{IR}$ ) of the symmetric methylene stretching band. Part c shows the COG of the carbonyl stretching and of the phosphate antisymmetric stretching bands. The arrows point to the respective coordinate axes. The lipid was polymerized in the  $L_\alpha$  state (RH = 50%,  $T = 25$  °C) using a wire grid to weaken the UV irradiation by  $\sim 30\%$ . Inserts. Part a: Plot of  $\ln\{-\ln(1 - F^P(t))\}$  as a function of  $\ln(t)$ , where  $t$  is the irradiation time. The slope and intercept of the linear regression yield  $n = 0.82$  and  $\tau_b = 103$  min. Part b: Correlation plot between COG( $\nu_s(\text{CH}_2)$ ) and  $F^P$ .

of time (see Figure 4, part a), respectively:

$$F^C(t) = \frac{A_{1603}(t)}{g_{1c}A_{1593}(0) + A_{1603}(0)}$$

$$F^T(t) = \frac{g_{1c} \cdot A_{1593}(t)}{g_{1c}A_{1593}(0) + A_{1603}(0)}$$

$$F^P(t) = 1 - (F^C(t) + F^T(t)) \quad (2)$$

Note that  $F^C$ ,  $F^T$  and  $F^P$  represent fractions of the total amount of acyl chains, whereas  $f^T$  (cf. eq 1) refers to “monomeric”

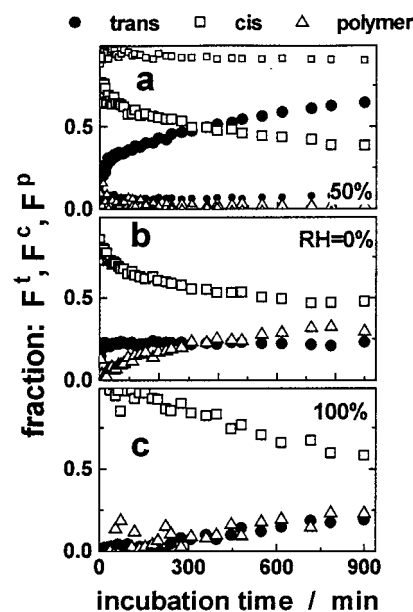


**Figure 5.** Fraction of trans (●) and cis (□) isomers and of polymeric (Δ) DTDPC ( $F^T$ ,  $F^C$ , and  $F^P$ , respectively) as a function of incubation time. The lipid was stored at RH = 0%, 50%, and 100% (parts a–c) and  $T = 50$  °C (except small symbols in part a that correspond to  $T = 5$  °C).

**TABLE 3: Kinetic Analysis of the UV Induced Polymerization of DTDPC and DTDPE at Different Conditions**

lipid	RH %	$T$ °C	$\Pi^d$ GPa	phase <sup>b</sup>	$\tau_1^a$ min	$\tau_2^a$ min	$n^c$	$\tau_n^c$ min
DTDPC	10	10	0.30	gel	6	37	0.51	11
	80	10	0.029	$L_\alpha$	9	102	0.61	38
	10	30	0.32	$L_\alpha$	8	40	0.51	6
	80	30	0.031	$L_\alpha$	13	51	0.73	32
DTDPE	50	15	0.093	$C_I$	3	32	0.49	8
	50	15	0.093	$C_{II}$	3	31	0.43	6
	50	50	0.103	$H_{II}$	4	29	0.62	17

<sup>a</sup> The time courses  $F^C(t)$ ,  $F^T(t)$ , and  $F^P(t)$  are fitted each by a biexponential function of the form  $a_1 \exp(-t/\tau_1) + a_2 \exp(-t/\tau_2)$  with the condition of equal decay times  $\tau_1$  and  $\tau_2$ . Note that for  $F^C(t)$  the preexponential factor  $a_2$  is negative. Standard error:  $\pm 2$  min ( $\tau_2$ ) and  $\pm 5$  min ( $\tau_1$ ). <sup>b</sup> Refers to the lipid monomer. <sup>c</sup> From linear fits of  $\ln\{-\ln(1 - F^P(t))\}$  versus  $\ln(t)$ . Standard error:  $\pm 0.03$  ( $n$ ),  $\pm 3$  min ( $\tau_n$ ). <sup>d</sup> Vapor pressure:  $\Pi = (-RT/\nu_w) \cdot \ln(RH/100)$ ;  $R$ , gas constant;  $\nu_w = 1.8 \times 10^{-5}$  m<sup>3</sup> mol<sup>-1</sup>, molar volume of water.<sup>5</sup>

tetradecadienoyl chains only. It should be emphasized that we cannot differentiate between both diene groups in each lipid molecule on the basis of the spectral parameters used. The fractions  $F^T$ ,  $F^C$ , and  $F^P$  (and also  $f^T$ ) represent mean values which are averaged over all acyl chains in the sample. There is, however, no experimental indication of a different polymerization and/or isomerization behavior of the diene groups in the *sn*-1 or *sn*-2 acyl chains of the lipid.

Figure 4, part a, depicts typical time courses of the fractions of monomeric and polymerized fatty acid residues of DTDPC existing in the liquid crystalline phase ( $L_\alpha$ ). For a first evaluation we fitted the experimental data empirically using biexponential functions with the decay times  $\tau_1$  and  $\tau_2$  ( $\tau_1 < \tau_2$ , see Table 3). The short decay time  $\tau_1$  is only weakly affected by the variation of the external conditions at which polymerization has been realized. However, the longer decay component  $\tau_2$  increases when the RH is increased. Polymerization at a higher temperature accelerates the conversion at longer times only at nearly full hydration of the lipid (RH = 80%). At RH = 10% and  $T = 10$  °C the lipid does not exist in the gel state. Obviously the phase of the lipid does not modify lipid polymerization at almost dry conditions (RH = 10%). The attenuation of the UV radiation

by means of a wire grid increases both decay times by nearly the same factor ( $\sim 3$  times, cf. caption of Figure 4).

Among other attempts (see, for example, ref 19) it seems appropriate to analyze the kinetics of polymerization in solid and fluid media in terms of the "stretched" exponential function<sup>9,20</sup>

$$F^p(t) = 1 - \exp\left[-\left(\frac{t}{\tau_n}\right)^n\right] \quad (3)$$

Analogous to crystal growth,<sup>21</sup> the exponent  $n$  characterizes topochemical features of polymerization with  $1 \leq n < 2$  for linear,  $2 \leq n < 3$  for platelike, and  $3 \leq n < 4$  for polyhedral growth. If diffusion processes, such as reorientation and/or translational motions of the molecules, are significantly involved in the reaction, the exponent adopts values  $n < 1$ . The experimental data are well fitted by linear regression when one plots  $\ln\{-\ln(1 - F^p(t))\}$  versus  $\ln(t)$  (see insertion in Figure 4, part a). The slope and intercept yield  $n$  and the time constant  $\tau_n$ , respectively (Table 3). The exponents  $0.4 < n < 0.75$  are typical for a diffusion controlled one-dimensional growth process as observed in other polymerization reactions as well.<sup>20</sup> Interestingly, the exponents are systematically bigger ( $\sim 0.6$ – $0.7$ ) in fluid, more hydrated films than in solid and/or nearly dry ones ( $\sim 0.4$ – $0.5$ ).

**Spontaneous Polymerization.** Thermal polymerization of DTDPC in the absence of initiating agents has been observed to proceed in vesicles within 600 min at  $T = 60^\circ\text{C}$  (95% conversion).<sup>12</sup> Upon storage of lipid films on the ATR crystal at  $\text{RH} < 20\%$  and  $\text{RH} > 99\%$  ( $T = 50^\circ\text{C}$ ), we observed a slight decrease of the total intensity of the  $\nu_{\text{as}}(\text{C}=\text{C})$  bands  $I_{\text{tot}}$ , which can be assigned to spontaneous polymerization as well. The data analysis in terms of eq 2 yields the fraction of polymerized acyl chains as a function of incubation time. At  $\text{RH} = 100\%$ , polymerization and isomerization proceed parallel (Figure 5, part c). In excess water and  $T = 50^\circ\text{C}$ ,  $F^1$  passes through a maximum and decreases at longer times indicating the conversion of both isomers to the polymer (data not shown). At  $\text{RH} = 0\%$ , the fraction of trans isomers of the monomer remains nearly constant (Figure 5 part b). Obviously only the cis isomer polymerizes and no significant cis/trans isomerization occurs. At intermediate RH, no significant polymerization can be detected (Figure 5, part a, i.e.,  $F^p < 0.1$ ).

This result is confirmed by the heating scans of two samples ( $\text{RH} = 10\%$ ), one of which was prepared using DTDPC with predominantly cis and the other by using DTDPC with predominantly trans isomers of the terminal diene groups (Figure 6). The sigmoidal courses of the center of gravity and of the IR order parameter of the symmetric methylene stretching band give evidence of a chain melting transition where the lipid transforms from the gel into the liquid-crystalline ( $L_\alpha$ ) phase. The negative  $S_{\text{IR}}(\nu_s(\text{CH}_2))$  values are typically observed in ATR measurements on lamellar samples where the lipid layers align parallel to the crystal surface (see, for example, refs 6 and 22).

First, we note that the sample of predominantly cis isomers undergoes the phase transition at more than  $\sim 10$  K below the sample of predominantly trans isomers. It is well-known that there are profound differences in the phase behavior of cis and trans unsaturated phospholipid analogues. For example, the gel/ $L_\alpha$  phase transition of fully hydrated trans di7:7t PC (DEPC) appears at  $+11^\circ\text{C}$ ,<sup>23</sup> whereas the cis analogue DOPC (di 7:7c PC) transforms at  $-16^\circ\text{C}$ .<sup>24</sup> The increase of the transition temperature in the former system can be rationalized by the bent geometry of the cis double bond which causes additional disorder within the hydrophobic core of the bilayers.<sup>25,26</sup>

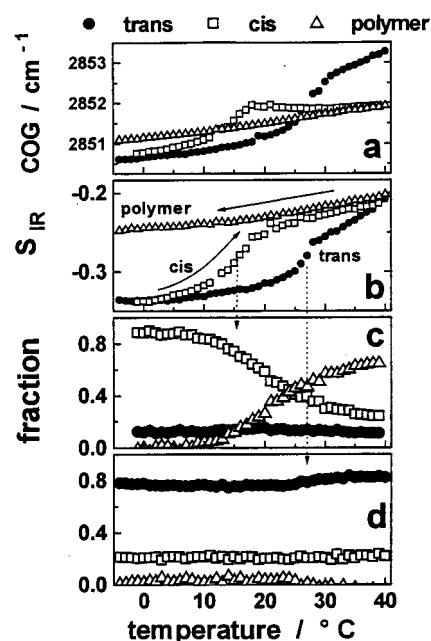


**Figure 6.** Center of gravity (COG, part a) and IR order parameter ( $S_{\text{IR}}$ , part b) of the  $\nu_s(\text{CH}_2)$  band, and the fractions of cis, trans, and polymeric DTDPC (parts c and d) as a function of temperature in lipid films which have been prepared using predominantly trans and cis isomers ( $\text{RH} = 10\%$ ). Note that parts c and d depict the composition of the latter (cis) and former (trans) sample, respectively, as indicated by the dotted arrows. The cis sample has been annealed for 2 h at  $T = 40^\circ\text{C}$  to complete polymerization before cooling (triangles, see text for discussion).

The correlation plot of the  $\text{COG}(\nu_s(\text{CH}_2))$  before and after cis  $\rightarrow$  trans isomerization given in Figure 7 (see next paragraph) indicates a slight decrease of this parameter upon isomerization which can be interpreted in terms of a slightly increased ordering in the hydrophobic core of the membranes of *trans*-DTDPC. The polar region of the membranes is not affected by the isomerization as demonstrated by the correlation plot of the position of the  $\text{C}=\text{O}$  stretching band (Figure 7). A detailed study of the phase behavior and structural details of the bilayers of both isomers of monomeric DTDPC will be given in a separate publication.

The second, more important finding in the context of lipid stability is the pronounced polymerization of the cis isomer which starts just at the onset of the gel/ $L_\alpha$  phase transition (cf. Figure 6, parts a–c). Also in this experiment the trans isomer remains essentially monomeric independent of its fraction. In other words,  $F^1$  is constant if the trans acyl chains constitute the minority (Figure 6, part c) or majority (Figure 6, part d) fraction in the mixture of both isomers. On the other hand, cis acyl chains do not polymerize if they are diluted in bilayers of a dominating trans fraction (Figure 6, part d).

To complete polymerization in films of predominantly *cis*-DTDPC, the respective sample was stored at  $T = 40^\circ\text{C}$  for 2 h. Reversed cooling shows that the phase transition in the polymerized film disappears completely (Figure 6, parts a and b). Note that the phase transition of *trans*-DTDPC is reversible (data not shown).

**Molecular Ordering Before and After Polymerization.** To study modifications of the molecular arrangement in the lipid aggregates we plot selected spectral parameters as a function of the irradiation time (see, for example Figure 4, parts b and c). It turns out that in the liquid-crystalline phase the polar part of the bilayer is only weakly affected by polymerization as indicated by the only slight changes of the centers of gravity



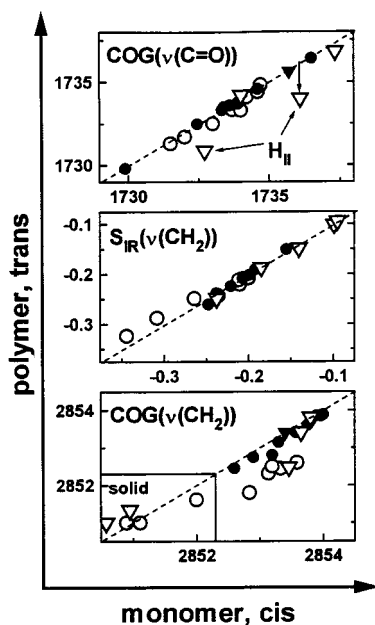


**Figure 7.** Autocorrelation plot of the IR parameters measured in lipid films before (horizontal axis) and after (vertical axis) UV polymerization (open symbols) and isomerization (solid symbols). Circles refer to DTDPC and triangles to DTDPE. The respective IR parameters are indicated in the figure. The diagonal lines correspond to invariant parameters.

of vibrational modes of the carbonyl and phosphate groups (Figure 4, part c). In contrast to this behavior the COG of the symmetric methylene stretching mode,  $\nu_s(\text{CH}_2)$ , decreases parallel to the increase of the mol fraction of polymerized lipid  $F^p(t)$  (Figure, 4 part b). The correlation plot of both parameters shown in the insertion of Figure 4 suggests that polymerization instantaneously modifies the properties of the hydrophobic core of the bilayer. On the other hand, polymerization does obviously not destroy the macroscopic orientation of the lipid bilayers as shown by the IR order parameter of the methylene segments  $S_{\text{IR}}(\nu_s(\text{CH}_2))$ , which remains essentially constant upon UV irradiation. (Figure 4, part b).

For a generalization of these findings we correlate the IR parameters measured in lipid films at different RH and  $T$  before polymerization with that obtained after polymerization (Figure 7). The correlation plots include data which correspond to bilayers of DTDPC in the  $L_\alpha$  and gel phases as well as to the inverse hexagonal phase and to the crystalline ( $C_1$  and  $C_{\text{II}}$ , see below) states of DTDPE.<sup>6</sup> As found for the example given in Figure 4, polymerization has only a small effect on the  $\text{C}=\text{O}$  stretching band with exception of the  $\text{H}_{\text{II}}$  phase of monomeric DTDPE. The significant shift of  $\text{COG}(\nu(\text{C}=\text{O}))$  toward smaller wavenumbers during polymerization indicates the increasing hydration of the carbonyl moieties. Similar changes of the  $\nu(\text{C}=\text{O})$  frequency has been observed at the  $\text{H}_{\text{II}}/L_\alpha$  phase transition of monomeric PEs.<sup>27–29</sup> We suggest that the shift of  $\text{COG}(\nu(\text{C}=\text{O}))$  is caused by the partial or complete destruction of the inverse hexagonal phase upon polymerization. Polymerization of the terminal ends of the lipid tails can be expected to perturb the  $\text{H}_{\text{II}}$  phase. A detailed study of this phenomenon will be given elsewhere. The polymerization of  $\text{H}_{\text{II}}$  aggregates has been realized successfully in systems of lipids with the reactive groups adjacent to the glycerol unit, i.e., in a position near the neutral plane of the aggregates.<sup>30</sup>

The position of the methylene stretching bands shifts systematically to smaller wavenumbers in all samples which are polymerized in the  $L_\alpha$  phase. The  $\nu_s(\text{CH}_2)$  frequency is sensitive

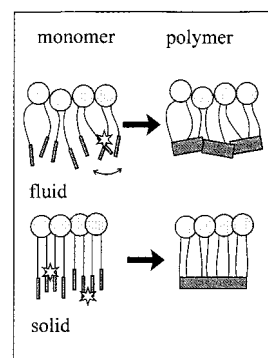


**Figure 8.** Schematic representation of lipid layers before and after polymerization. Only one-half of the bilayer is shown. The diene groups are symbolized by small rectangles (left) and the polymeric network by bigger ones (right). The double arrow indicates reorientational motions of the diene groups and the stars reactions between diene groups in a favorable orientation and position each to another (see text).

to the chemical nature of the atomic groups adjacent to a methylene unit. It can differ by more than  $10 \text{ cm}^{-1}$  when comparing the  $\alpha$ - and  $\omega$ -methylenes in fatty acid residues and  $n$ -alkanes.<sup>31–33</sup> From the chemical point of view, polymerization of the terminal diene groups is expected to modify the terminal vinyl groups and the methyne groups adjacent to the  $\omega$ -methylene groups. The  $\text{COG}(\nu_s(\text{CH}_2))$  represents a mean frequency averaged over the individual modes of 22 methylene units per DTDPC/PE molecule before and of 24 methylenes after polymerization. The considerable shift of the  $\text{COG}(\nu_s(\text{CH}_2))$  upon polymerization can hardly be explained by the variation of only four of them. In addition we found that the COG of the antisymmetric methylene stretching vibration,  $\nu_{\text{as}}(\text{CH}_2)$ , shifts nearly parallel to the  $\text{COG}(\nu_s(\text{CH}_2))$  from  $\sim 2923 \text{ cm}^{-1}$  down to  $\sim 2921 \text{ cm}^{-1}$  (data not shown). This finding gives evidence that band overlap effects can be ruled out to explain the frequency shifts of the  $\text{CH}_2$  stretching bands because it would affect both  $\text{CH}_2$  modes differently. On the other hand, the position of the  $\nu_s(\text{CH}_2)$  and  $\nu_{\text{as}}(\text{CH}_2)$  bands are sensitive to the conformational order of the acyl chains (vide supra).<sup>34–36</sup> We suggest that the downward shift of  $\text{COG}(\nu_s(\text{CH}_2))$  indicates a more rigid arrangement of the acyl chains after polymerization (see Figure 8 for illustration). Intermolecular covalent bonds in the center of the hydrophobic core of the bilayers can be expected to restrict the conformational freedom of the methylene segments distinctly.

The nearly invariant IR order parameter of the methylene segments  $S_{\text{IR}}(\nu_s(\text{CH}_2))$  (Figure 7) seems to contradict this hypothesis. One can, however, assume that polymerization fixes a particular structure of the polymethylene chains and thus freezes up the degree of disorder within the hydrophobic region of the monomeric aggregates in the moment of the reaction. In addition, the IR order parameter can be written as the product of the local molecular order parameter  $S_\mu$  and the order parameter of the local director with respect to the ATR surface  $S_d$ , i.e.,  $S_{\text{IR}} = S_d S_\mu$ .<sup>6</sup> The more fluid the monomeric aggregates the smaller  $S_d$  because of undulations and curved regions of the membranes. Polymerization can be assumed to fix the degree of macroscopic ordering. Bilayers which are polymerized in the fluid state obviously fit less perfectly on the ATR surface than membranes which are polymerized in the highly ordered gel state.

Studies on lipids with terminal sorbyl groups suggest that the reactive groups in the  $sn$ -1 tails react preferentially each with another to form polymer chains.<sup>37</sup> Then, cross links between these polymer chains occur when a reactive group on



the *sn*-2 tail in one polymer chain reacts with a similar group in a neighboring polymer chain. The selectivity of the polyreaction appears plausible in view of the inequivalent packing of the two acyl chains per lipid which causes the polymerizable groups in the *sn*-1 tail to penetrate further toward the bilayer center than that in the *sn*-2 tail. The IR linear dichroism of the C—O—C ester bond vibration of monomeric DTDPC and DTDPE lamellae gives evidence of the structural inequivalence of the *sn*-1 and *sn*-2 tetradecenoyl chains.<sup>6</sup> We suggest that UV-induced polymerization of diene lipids proceeds in the same cross-linking manner within the supported films studied as in the bilayers of PCs with terminal sorbyl groups. This conclusion is confirmed by the stability of the product (*vide supra*) and by the nearly invariant dichroism of the C—O—C stretching bands of the polymer when compared with that of the monomer (data not shown). This finding shows that the inequivalent packing of the *sn*-1 and *sn*-2 chains is obviously fixed by the covalent bonds between the lipid molecules. The cross-linked polymer chains can be thought to resemble 1,4-*trans*-polybutadiene at least partially as has been proposed previously for polymerized vesicles and monolayers of diene lipids.<sup>3,38</sup> In addition, the partial interdigitation of the terminal diene groups in the center of the bilayer can produce monolayer-to-monolayer covalent bonds which have been suggested to appear in polymerized bilayers of DTDPC.<sup>12,39</sup> On the other hand, segmental disorder and packing defects of the hydrocarbon chains will prevent the formation of a regular polymer network. For example, bis-PC links from the *sn*-1 group in one polymeric chain to a *sn*-2 group in a second chain and/or intramolecular macrocyclization of the *sn*-1 and *sn*-2 groups in the same lipid are possible. One can expect an increasing degree of irregularity of the polymeric network if the polymerization has been performed within more fluid membranes. Consequently, the observed correlation between the mean order parameter of the CH<sub>2</sub> groups before and after polymerization can be interpreted in terms of the degree of regularity of the polymeric network formed. The kinetic analysis confirms this hypothesis qualitatively (see below).

**Polymerization in the Solid State.** Polymerization of diene lipids in vesicles is temperature-dependent, the degree of polymerization being higher when the lipid exist in the L<sub>α</sub> phase.<sup>1</sup> This is in contrast to diacetylene lipids which can only be polymerized in the gel state where the diacetylene groups correctly align.<sup>3</sup> On the other hand, solid films of long chain butadiene derivatives convert into highly stable crystalline 1,4-*trans*-butadiene with a high yield upon UV irradiation.<sup>18</sup> In this case strong hydrogen bonding between the molecules can influence the specific course of the polymerization reaction.

These facts raise interest to study details of solid state polymerization of diene lipids with terminal diene groups which can exist in several rigid states, namely, the gel (DTDPC and DTDPE) and two crystalline polymorphs of DTDPE.<sup>6</sup> A series of nearly equally spaced absorption bands appears in the spectral range 1340–1205 cm<sup>-1</sup> in all solid samples. It can be assigned to the methylene wagging band progression the prominent  $\gamma_w(\text{CH}_2)^1$  mode of which protrudes at  $\sim 1205$  cm<sup>-1</sup> (see Figure 9 small arrows). This feature is an indicative signature of the fact that the polymethylene fragments of the tetradecenoyl chains exist mainly in the extended all-*trans* conformation. In the gel state, the frozen acyl chains are packed in a hexagonal lattice and randomly oriented with respect to rotations about the chain axes. Strong intermolecular interactions between the PE headgroups in the DTDPE crystals force the acyl chains to pack into paraffin-like subcells where the planes of neighboring polymethylene chains tend to align either parallel (C<sub>II</sub> crystalline

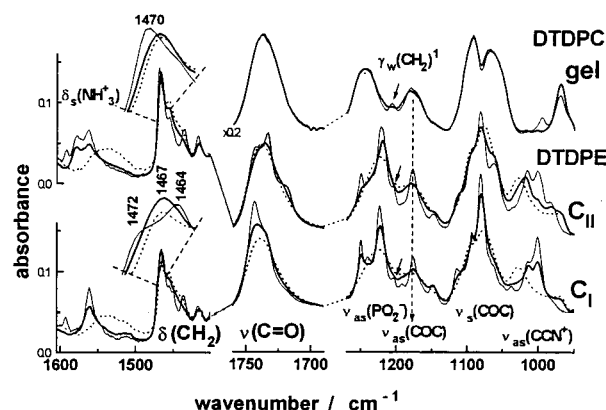


**Figure 9.** Selected regions of the infrared absorbance spectra of DTDPC (above) and of DTDPE (below) before (thin solid lines) and after (thick solid lines) UV irradiation for 30 min in the rigid states (see figure for assignment of the phase state). The conditions are RH = 10% and  $T = 10$  °C (DTDPC) and RH = 50% and  $T = 15$  °C (DTDPE). The dotted curves are recorded at RH = 50% and 25 °C after incubation of the DTDPE samples at RH = 98% (see text). Selected absorption bands are assigned in the figure (see ref 6 for a detailed assignment). The peak region of the  $\delta(\text{CH}_2)$  band is enlarged.

polymorph) or perpendicularly (C<sub>I</sub>). This different arrangement of the acyl chains becomes evident in the shape and position of the methylene bending band,  $\delta(\text{CH}_2)$ , which represents clearly a doublet in the C<sub>I</sub> form owing to crystal field splitting in an orthorhombic perpendicular (O<sub>⊥</sub>) lattice (Figure 9, left part). In contrast, a narrow  $\delta(\text{CH}_2)$  band which is centered at relatively high wavenumbers ( $\sim 1470$  cm<sup>-1</sup>) is observed in the C<sub>II</sub> form. It appears typically in paraffin subcells with parallel methylene planes.<sup>40</sup> Note that the maximum of the  $\delta(\text{CH}_2)$  band of the lipid in the gel state is located at  $\sim 1467$  cm<sup>-1</sup>.

Upon UV polymerization, the wagging band progression vanishes. Obviously the newly formed structure is characterized by defects of the all-*trans* conformation of the polymethylene chains which depress the vibrational coupling between adjacent methylene units (see Figure 8 for illustration). Moreover, the specific features of the  $\delta(\text{CH}_2)$  mode of the DTDPE crystals transform into a single band at  $1467$  cm<sup>-1</sup>. This finding shows that the transverse ordering of the acyl chains is completely destroyed. Note that the COG and the IR order parameter (only DTDPC) of the  $\nu_s(\text{CH}_2)$  band increase slightly upon polymerization in accordance with these findings (see Figure 7). The respective data differ however considerably from the values measured typically in the liquid-crystalline phase of the monomeric lipids indicating a higher degree of ordering in the hydrophobic core of the aggregates which are polymerized in the rigid state. Note that solid state polymerization proceeds relatively fast when compared with fluid hydrated systems (Table 3).

Interestingly, the crystalline characteristics of the PE head-group remain essentially unaltered during UV irradiation. In particular, the  $\delta_s(\text{NH}_3^+)$  and  $\nu_{\text{as}}(\text{CCN}^+)$  modes of the choline group and the  $\nu_{\text{as}}(\text{PO}_2^-)$  vibration of the phosphate group are typical for the respective polymorphs of DTDPE (see ref 6 for assignments). The absorption bands of the carbonyl-ester moiety,  $\nu(\text{C=O})$  and  $\nu_{\text{as}}(\text{COC})$ , are affected to an intermediate extent, i.e., they broaden distinctly but maintain some specific properties of the crystals (e.g. the maximum position of  $\nu(\text{C=O})$ ). Thus, the more distant a moiety from the center of the bilayer the smaller the spectral changes and consequently, the smaller the modification of the crystalline structure. The crystalline head-group arrangement of the polymer can be broken up if one hydrates the polymerized crystals up to RH > 85% ( $T = 25\%$ ).

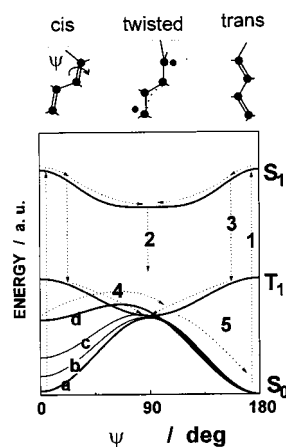


**Figure 10.** Schematic representation of the energy of the ground ( $S_0$ ) and excited ( $S_1$ ) singlets and of the triplet state ( $T_1$ ) of a terminal diene group as a function of the torsion angle  $\psi$  for rotations about the inner double bond (see upper part of the figure). The shape and relative position of the curves is adopted from the respective dependencies given in refs 41 and 42 which are calculated for isolated butadiene including bond length relaxation in the perpendicular conformation. The curves b–d visualize hypothetical changes of the  $S_0$  energy at increasing RH (see text). Corresponding changes of the  $S_1$  and  $T_1$  energies are omitted.

Note that crystals of monomeric DTDPE transform into the fluid phase at nearly identical conditions. In the latter case this process is accompanied by a considerable increase of the IR order parameter of the methylene stretching bands indicating the melting of the acyl chains (e.g.,  $\Delta S_{\text{IR}}(\nu_s(\text{CH}_2)) > 0.1$ ). In the polymerized systems only tiny changes of  $S_{\text{IR}}(\nu_s(\text{CH}_2))$  ( $< 0.04$ ) and  $\text{COG}(\nu_s(\text{CH}_2))$  are found due to the high degree of ordering in the hydrophobic core which is not affected by structural modifications in the polar region. The nearly identical conditions in monomeric and polymeric films at which the crystalline headgroup structure is broken up shows that the stability of DTDPE crystals is determined mainly by the interactions between the PE moieties. The melting of polymerized DTDPE crystals was found to be irreversible. After reversed dehydration the spectra of the DTDPE polymer look very alike as those of monomeric DTDPE in the gel state (see Figure 7, dotted curves and ref 6). Note that the headgroup and carbonyl vibrations of the PC analogue DTDPC are essentially not affected by polymerization (Figure 7).

#### 4. Discussion

**Energetic Features of Diene Groups Dependent on the Torsion about Double Bonds.** The hypothetical dependence of singlet ground ( $S_0$ ), excited ( $S_1$ ), and triplet ( $T_1$ ) optimized energies of the diene group on the torsion angle about the internal double bond  $\psi$  is depicted in Figure 10 assuming similar courses as calculated for butadiene.<sup>41,42</sup> The barrier to rotations about the double bonds of isolated dienes in the ground state ( $\sim(130\text{--}250)$  kJ/mol<sup>14,43,44</sup>) exceeds the barrier for rotations about the single bond ( $\sim(10\text{--}20)$  kJ/mol) by more than 1 order of magnitude, and thus cis  $\rightarrow$  trans isomerization in the ground state is practically impossible for dienes which are dissolved in a solvent of low viscosity. It can however be realized by UV absorption (process 1 in Figure 10) via the rapid relaxation of the cis or trans excited state to a twisted intermediate in both the singlet and triplet manifolds (2 and 3) which can decay to the ground state of both isomers (5). Typically an increase in the solvent viscosity retards the trans/cis process selectively while allowing the reverse process to proceed.<sup>10</sup> The viscosity effect has been rationalized in terms of an increase in the

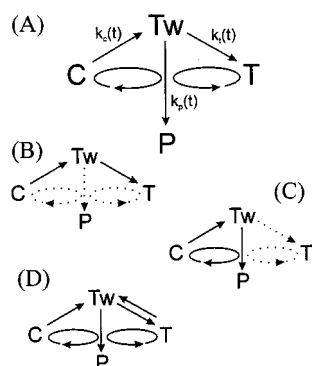
molecular volume along the reaction path of the trans  $\rightarrow$  cis isomerization because of the different sizes of both isomers. In lipid membranes the cis  $\rightarrow$  trans process could result in a relaxation, or at least it should encounter little resistance, while the reverse trans  $\rightarrow$  cis process should be an expansion, sterically restricted in the semirigid environment. Owing to the bent geometry of cis unsaturation, the cis isomer is more bulky than the trans isomer and thus it introduces additional disorder into the hydrophobic core. As a result, the cis isomer gives rise to a local minimum of energy whereas the trans isomer refers to the global minimum because it fits well into the parallel aligned acyl chains (Figure 10). It has been found that, for example, 1,3-butadiene when incorporated in a nematic matrix adopts preferentially the s-trans conformation and orients with the long molecular axis parallel to the nematic director.<sup>45</sup> Hence, the UV-induced cis  $\rightarrow$  trans isomerization of the diene groups of DTDPC, DTDPE, and 9,11-DODPC can be assumed to proceed by a similar mechanism as that which occurs upon irradiation of cis olefins in monolayer film assemblies.<sup>10</sup> It results in a rapid and irreversible conversion to the trans isomer.

The spontaneous cis  $\rightarrow$  trans isomerization of the terminal diene groups (process 4 in Figure 10) occurring during storage of the lipid films can be explained if the relative height of the barrier for the cis  $\rightarrow$  trans rotation is decreased to a value which is comparable with the activation energies measured (45–65 kJ/mol). As discussed above dehydration of the lipids causes an increasing osmotic stress which can be expressed in terms of the vapor pressure  $\Pi$  acting effectively on the lipid aggregates. Upon compression, the molecular ordering within the hydrophobic core increases and the local energy minimum of the bulky cis isomer can be suggested to increase relative to the energy maximum of the twisted conformation. Ultimately the effective barrier height decreases (see curves a–d in Figure 10 for illustration). The increasing vapor pressure (i.e., decreasing RH) has been found to accelerate isomerization at RH  $> 50\%$ . This behavior is reflected in the negative activation volume which is typical for condensation reactions where the density of the sample increases during the transformation. In a lipid bilayer the cis  $\rightarrow$  trans transformation can be suggested to reduce mainly the cross section of the molecules parallel to the polar/apolar interface of the aggregates. cis double bonds of diene groups in the mid position of the acyl chains are stable as found for 9,11-DODPC. Obviously the high mobility of the terminal diene groups of DTDPC and DTDPE is essential for spontaneous isomerization.

**Radical Formation and Polymerization.** In the perpendicular, twisted conformation the ground state becomes biradical.<sup>42</sup> The length of the C=C bond under torsion increases whereas the lengths of the remaining bonds in the C=C–C fragment approach each other. Also the relaxed geometrical structure of the  $S_1$  and  $T_1$  states corresponds to a twisted, biradical structure in which the two unpaired electrons tend to be pushed to the extremities of the conjugated  $\pi$  system since the torsion defines two delocalized radicals.<sup>41</sup> Hence, cis  $\rightarrow$  trans isomerization via a twisted intermediate in  $S_0$ ,  $S_1$ , and  $T_1$  states gives rise to transient radicals which can initiate polymerization of butadiene derivatives according to, for example, a 1,4-addition mechanism.<sup>8</sup> Consequently, isomerization and polymerization are closely related properties of diene groups in accordance with the experimental facts presented.

The short lifetime of the  $S_1$  state ( $\sim 10^{-10}$  s) precludes its productive involvement into polymerization.<sup>11</sup> The energies of the triplet and ground-state singlet are nearly degenerate for the twisted conformation.<sup>41</sup> For a straightforward interpretation of

## SCHEME 1



the possible reaction paths let us therefore consider one twisted, radical intermediate (Tw) which belongs to  $S_0$  or  $T_1$ , the cis and trans conformations in the ground state (C and T), and the polymer (P) (cf. Scheme 1).

In the general case (A), cis  $\rightarrow$  trans isomerization proceeds via the twisted radical which induces the addition of monomers to form the polymer. We suggest that this situation corresponds to liquid crystalline lipid films stored in a nearly saturated vapor atmosphere (RH  $\approx$  100%) or excess water. Note that also monoradicals as  $\cdot\text{OH}$  can start the polyreaction.<sup>46</sup> Chain growth via monoradicals should be interfered with by oxygen, causing formation of ether and/or peroxide linkages. No indications of such products could be detected in the IR spectra.

(B) In the intermediate RH range spontaneous cis  $\rightarrow$  trans isomerization proceeds without significant polymerization. Possibly the lifetime of the twisted intermediate is too short for interactions which cause polymerization. The particular factor why polymerization proceeds in case A but stops in case B is unknown.

(C) At nearly dry conditions (RH < 20%), the cis isomer polymerizes whereas the trans isomer remains essentially monomeric. As discussed above, the more bulky cis and twisted conformations become progressively unfavorable in an energetic sense. As a result the energetic maximum of the twisted state can be thought to increase and even to exceed the respective energy of the  $T_1$  state (cf. curve d in Figure 10). We suggest that a certain amount of originally cis isomers can transform to the triplet state by intersystem crossing when reaching the twisted conformation. Owing to its long lifetime ( $\sim 10^{-2}$  s<sup>11</sup>) the probability of polymerization is expected to increase considerably. Moreover, we suggest that the compression of the lipid aggregates at high vapor pressure causes a closer approach of the molecules and thus increases the probability to cross a threshold distance for the addition reaction. In general, unsaturated molecules become unstable at high pressure with respect to associative, cross-linking reactions which form denser, more saturated species.<sup>20</sup> For example this mechanism accelerates polymerization of acetylene under hydrostatic pressure.<sup>9</sup> In the solid state of the lipids molecular motions within the hydrophobic core including rotations about the chemical bonds of the diene backbone are frozen up and consequently no isomerization and polymerization takes place.

(D) Upon UV irradiation, both the cis and trans isomers can reach the twisted intermediate via the  $S_1$  state and subsequently polymerize as discussed above.

**Kinetics.** The reaction Scheme 1 considers two reaction paths,  $C \rightarrow Tw \rightarrow T$  and  $(C,T) \rightarrow Tw \rightarrow P$ , corresponding to isomerization and polymerization, respectively. Photoisomerization can be viewed effectively as a unimolecular reaction because all processes leading to the intermediate state as

absorption, nonradiative relaxation and intersystem crossing are fast ( $< 10^{-3}$  s) in comparison with the time resolution of the experiment (minutes). Also UV-induced polymerization of lipid vesicles at steady-state illumination has been shown to obey effectively unimolecular kinetics for similar reasons, i.e., reactive free radicals develop virtually instantaneously from the initial excited-state population.<sup>11</sup> The corresponding characteristic time for polymerization,  $\tau_p$ , is inversely proportional to the intensity of the UV light, i.e.,  $\tau_b = 1/(KI_{UV})$ . The constant  $K$  depends on the UV extinction coefficient of the diene groups ( $\epsilon_{UV}$ ), the yield of radical formation from excited species ( $\phi_r$ ), and the yield of polymer formation from radicals ( $\phi_p$ ), i.e.,  $K = \epsilon_{UV}\phi_r\phi_p$ .

Unimolecular reactions in amorphous polymers or membranes very often follow nonmonoexponential kinetics.<sup>19</sup> The origins of this behavior are the nonhomogeneous microenvironment around each reacting molecule and the fact that the matrix relaxes from the nonequilibrium situation or changes configuration in comparable or longer time scales than the reaction kinetics. In the DTDPC/DTDPE films we observed a response of the ordering and arrangement of the acyl chains which accompanies the polymerization process. Moreover, polymerization involves the reaction between radicals and ground-state monomers giving rise to a time-dependent propagation term which depends on the decreasing concentration of monomeric species.<sup>11</sup> Hence, it appears not surprisingly that isomerization and UV polymerization kinetics of DTDPC/DTDPE are nonmonoexponential. To consider this fact we express the respective rate constants as functions of time (Scheme 1). For a simple empirical approach of data reduction we fitted the time courses by two-exponential function. In agreement with the relation given in the previous paragraph, the time constants of polymerization  $\tau_1$  and  $\tau_2$  change proportional to the UV intensity, i.e., radical formation via the excited-state  $S_1$  is indeed rate limiting. The variation of the activation energies and volumes with incubation time reflects the nonmonoexponential character of the kinetics of spontaneous isomerization and, thus, should be interpreted as an approximate measure of the energetic barriers for this process.

For a physical interpretation of the UV polymerization kinetics we used the "stretched" exponential function (eq 3) which has been proved to accurately describe the kinetics in many cases. A rate equation of this type can be deduced in different ways, taking into account that many relaxation modes with different characteristic times contribute. For example, polymerization in condensed media can be thought to proceed via an idealized two-step mechanism: (a) transport of the reactants to the reactive sites by means of translational or rotational diffusion and (b) breaking and/or forming of chemical bonds.<sup>20</sup> Diffusion-controlled reaction kinetics where mechanism a is rate limiting obey typically "stretched" exponential functions with  $n \sim 0.5$ .

Consequently, the exponentials listed in Table 3 imply that the polymerization rate  $k_p(t)$  is controlled by a diffusion step preceding the reaction. We suggest that adjacent diene groups only react if they are in a favorable orientation and position to another (see Figure 8 for illustration). The mutual orientations of the diene groups can be assumed to span a certain range the width of which correlates with the degree of molecular ordering within the hydrophobic core. In most situations, neighboring diene groups encounter in a favorable position for reaction on the average only after several reorientations. The smaller the ordering of the diene orientations the smaller the probability to react within a given time interval, i.e.,  $k_p(t)$ , is expected to decrease with the order parameter of the acyl chains and vice



versa. In an assembly of frozen, tightly packed acyl chains also the diene groups can be suggested to arrange more regularly and polymerization proceeds faster than in a fluid bilayer where the diene groups are disordered to a higher degree. Interestingly, dehydration of fluid membranes also accelerates polymerization possibly due to the increasing molecular ordering within the hydrophobic core.

On the other hand, spontaneous isomerization (case B in Figure 10) has been found to proceed faster in a more fluid environment and to stop within solid lipid phases. That means the formation rate of the twisted intermediate  $k_c(t)$  decreases with increasing ordering of the acyl chains. The reaction path for spontaneous polymerization (case C) involves  $k_c(t)$  and  $k_p(t)$  which depend contrarily on the degree of molecular ordering. From the fact that the rates of spontaneous polymerization and isomerization depend in a similar fashion on molecular ordering one can conclude that  $k_c(t)$  is rate limiting in the spontaneous  $C \rightarrow Tw \rightarrow P$  conversion, i.e.,  $k_p(t) \gg k_c(t)$ . The nearly complete polymerization of the twisted intermediate (case C) can be explained if the formation rate of the trans isomer from the Tw state possesses the same order of magnitude as  $k_c(t)$ , i.e.,  $k_t(t) \approx k_c(t) \ll k_p(t)$ . The medium sensitivity of  $k_c(t)$  is manifested also in the circumstance that spontaneous polymerization obviously not occurs in a membrane where trans isomers constitute the major fraction. That is,  $k_c(t)$  obviously decreases with increasing  $f^t$ , possibly due to the denser packing of the trans isomers which progressively retards the remaining cis isomers to form twisted intermediates.

## 5. Conclusion

The most interesting result is that terminal diene groups undergo spontaneous cis/trans isomerization in lipid assemblies. Isomerization and polymerization are closely related properties of these moieties because they seem to proceed via a common twisted intermediate state. The isomerization and polymerization process can be triggered and controlled by the relative humidity of the atmosphere surrounding the lipid films. Lipid hydration controls reactive pathways within the hydrophobic region of the aggregates mainly by variations of the molecular ordering of the acyl chains. Polymerization of solid lipid phases destroys the crystalline packing of the acyl chains and causes conformational defects between the methylene units. It gives rise to well oriented polymerized multilayers on the solid support.

The effect of the cis and trans unsaturation on the ordering of the diene groups within the center of the hydrophobic core will be attacked in a separate publication. Further studies are directed to characterize the polymeric network and the dimensions and hydration properties of the polymerized membranes.

**Acknowledgment.** We thank Dr. M. Findeisen for recording the NMR spectra and Mrs. Dr. G. Lantzsch for producing the UV absorption spectroscopy. We would also to thank Prof. G. Klose and Prof. P. Welzel for the valuable comments on the manuscript and for discussions. This work was supported by the Deutsche Forschungsgemeinschaft under Grant of SFB294 and by BMBF under Grant 3DUBLEI-0.

## References and Notes

- (1) Blume, A. *Chem. Phys. Lipids* **1991**, 57, 253.
- (2) Chupin, V. V.; Anikin, A. V.; Serebrennikova, G. A. *Biol. Membr.* **1994**, 7, 213.

- (3) Hupfer, B.; Ringsdorf, H.; Schupp, H. *Chem. Phys. Lipids* **1983**, 33, 355.
- (4) Ohno, H.; Ogata, Y.; Tsuchida, E. *Macromolecules* **1987**, 20, 929.
- (5) Binder, H.; Anikin, A.; Kohlstrunk, B.; Klose, G. *J. Phys. Chem. B* **1997**, 101, 6618.
- (6) Binder, H.; Anikin, A.; Lantzsch, G.; Klose, G. *J. Phys. Chem. B* **1999**, 103, 461.
- (7) Whitten, D. G. *J. Am. Chem. Soc.* **1974**, 96, 594.
- (8) Tieke, B.; Wegner, G. *Makromol. Chem. Rapid Commun.* **1981**, 2, 543.
- (9) Aoki, K.; Usuba, S.; Yoshida, Y.; Kakudate, Y.; Tanaka, K.; Fujiwara, S. *J. Chem. Phys.* **1988**, 89, 529.
- (10) Kalyanasundram, K. *Photochemistry in Microheterogeneous Systems*; Harcourt Brace Jovanovich: New York, 1987.
- (11) Reed, W.; Guterman, L.; Tundo, P.; Fendler, J. H. *J. Am. Chem. Soc.* **1984**, 106, 1897.
- (12) Anikin, A.; Chupin, V.; Anikin, M.; Serebrennikova, G.; Tarahovsky, J. *Makromol. Chem.* **1993**, 194, 2663.
- (13) Anikin, A. V.; Anikin, M. V.; Vaislenko, I. A.; Orekhova, L. L.; Prokhorov, V. V.; Klinov, D. V.; Demin, V. V.; Barsukov, L. L. *Mendeleev Commun.* **1997**, 219.
- (14) Compton, D. A. C.; George, W. O.; Maddams, W. F. *J. Chem. Soc., Perkin Trans. 2* **1977**, 1311.
- (15) Segre, A. L.; Zetta, L.; Di Corato, A. *J. Mol. Spectrosc.* **1969**, 32, 296.
- (16) Rand, P. *Annu. Rev. Biophys. Bioeng.* **1981**, 10, 277.
- (17) Takeoka, S.; Iwai, H.; Ohno, H.; Tsuchida, E. *Bull. Chem. Soc. Jpn.* **1989**, 62, 102.
- (18) Tieke, B.; Wegner, G. *Colloid Polym. Sci.* **1985**, 263, 965.
- (19) Levitus, M.; Talhavini, M.; Negri, R. M.; Dib Zambon Atvars, T.; Aramendia, P. F. *J. Phys. Chem. B* **1997**, 101, 7680.
- (20) Yoo, C.-S.; Nicol, M. *J. Phys. Chem.* **1986**, 90, 6732.
- (21) Avrami, M. *J. Chem. Phys.* **1940**, 8, 212.
- (22) Fringeli, U. P.; Günthard, H. H. *Mol. Biol., Biochem. Biophys.* **1981**, 31, 270.
- (23) Chia, N.-C.; Mendelsohn, R. *J. Phys. Chem.* **1992**, 96, 10543.
- (24) Ulrich, A.; Sami, M.; Watts, A. *Biochim. et Biophys. Acta* **1994**, 1191, 225.
- (25) Siminovitch, D. J.; Wong, P. T. T.; Mantsch, H. H. *Biochemistry* **1987**, 26, 3277.
- (26) Wong, P. T. T.; Siminovitch, D. J.; Mantsch, H. H. *Biochim. et Biophys. Acta* **1988**, 947, 139.
- (27) Cheng, K. H. *Chem. Phys. Lipids* **1991**, 60, 119.
- (28) Mantsch, H. H.; Martin, A.; Cameron, D. G. *Biochemistry* **1981**, 20, 3138.
- (29) Castresana, J.; Nieva, J.-L.; Rivas, E.; Alonso, A. *Biochem. J.* **1992**, 282, 467.
- (30) Srisiri, W.; Sisson, T. M.; O'Brien, D. F. O.; McGrath, K. M.; Han, Y.; Gruner, S. M. *J. Am. Chem. Soc.* **1997**, 119, 4866.
- (31) MacPhail, R.; Strauss, A. H.; Snyder, L. R.; Elliger, A. C. *J. Phys. Chem.* **1984**, 88, 334.
- (32) Hill, I. R.; Levin, I. W. *J. Chem. Phys.* **1979**, 70, 842.
- (33) Bansil, R. J.; Day, J.; Meadows, M.; Rice, D.; Oldfield, D. *Biochemistry* **1980**, 19, 1938.
- (34) Casal, H. L.; Mantsch, H. H. *Biochim. Biophys. Acta* **1984**, 779, 381.
- (35) Snyder, R.; Strauss, H. L.; Elliger, C. A. *J. Phys. Chem.* **1982**, 86, 5145.
- (36) Kodati, V. R.; Lafleur, M. *Biophys. J.* **1993**, 64, 163.
- (37) Sisson, T. M.; Lamparski, H. G.; Kölchens, S.; Elayadi, A.; O'Brien, D. F. *Macromolecules* **1996**, 29, 8321.
- (38) Hupfer, B.; Ringsdorf, H.; Schupp, H. *Makromol. Chem. Rapid Commun.* **1981**, 182, 247.
- (39) Gordelij, V. I.; Cherezow, V. G.; Anikin, A. V.; Anikin, M. V.; Chupin, V. V.; Teixeira, J. *Prog. Colloid Polym. Sci.* **1996**, 100, 338.
- (40) Holland, R. F.; Nielsen, J. R. *J. Mol. Spectrosc.* **1962**, 8, 383.
- (41) Said, M.; Maynau, D.; Malrieu, J.-P. *J. Am. Chem. Soc.* **1984**, 106, 580.
- (42) Said, M.; Maynau, D.; Malrieu, J.-P.; Garcia Bach, M.-A. *J. Am. Chem. Soc.* **1984**, 106, 571.
- (43) Compton, D. A. C.; George, W. O.; Maddams, W. F. *J. Chem. Soc., Perkin Trans. 2* **1976**, 1666.
- (44) Lasaga, A. C.; Aerni, R. J.; Karplus, M. *J. Chem. Phys.* **1980**, 73, 5230.
- (45) Segre, A.; Castellano, S. J. *Magn. Reson.* **1972**, 7, 5.
- (46) Ohno, H.; Ogata, Y.; Tsuchida, E. *J. Polym. Sci. A* **1986**, 24, 2959.